XV International Conference on Durability of Building Materials and Components
DBMC 2020, Barcelona
C. Serrat, J.R. Casas and V. Gibert (Eds)

Field Study on Hydrophobised Internally Insulated Masonry Walls

Evy Vereecken, Daan Deckers, Hans Janssen and Staf Roels

KU Leuven, Department of Civil Engineering, Building Physics Section, Kasteelpark Arenberg 40, 3001 Leuven, Belgium, Evy.Vereecken@kuleuven.be

Abstract. *This paper presents a field study on the hygrothermal performance of hydrophobised masonry walls, provided with vapour tight or capillary active interior insulation. As a reference, also non-hydrophobised and non-insulated walls are analysed. To study the hygric performance, apart from traditional relative humidity sensors, in-house made moisture pins are embedded in the walls and are shown to yield valuable information in the high moisture range. Attention is given to the hygric performance of the wooden beam heads, the impact of wind-driven rain on the moisture conditions in the masonry wall, as well as to the impregnation depth of the water repellent agent. For the latter, the field study is supplemented with X-ray and liquid droplet measurements on a small semi-duplicate test wall. During the hydrophobisation process, an increased moisture level was induced. A drying period was needed to again reduce this level. After this period, a hydrophobic treatment showed a positive impact on the wall's hygric performance. The non-hydrophobised wall with a vapour tight interior insulation system showed the highest moisture level, especially deeper in the wall and thus where the wooden beam ends are located.*

Keywords: *Internally Insulated Masonry, Hydrophobisation, Hygrothermal Performance, Wooden Beams, Moisture Pins.*

1 Introduction

Driven by energy concerns and stricter energy regulations, wall insulation gains increasing importance. When dealing with renovation projects, three post-insulation techniques make a thermal upgrade of existing walls possible, i.e. cavity wall insulation, exterior insulation or interior insulation. For massive masonry walls with a valuable exterior facade, however, interior insulation remains as the only option. Unfortunately, interior insulation often leads to higher moisture contents in the wall, increasing the risk on wood rot of embedded wooden beam ends, frost damage, etc. (Vereecken *et al.*, 2015). These damage patterns are to a large extent caused by an exterior moisture source such as wind-driven rain (WDR), and therefore the application of a hydrophobic treatment is often pushed forward. To correctly estimate the effectiveness and potential side effects of a hydrophobic treatment, however, more insight on the moisture transport in hydrophobised walls is required. Thereto, this paper presents the results of a field study on the hygrothermal performance of hydrophobised internally insulated masonry walls.

Both walls with a vapour tight and with a capillary active interior insulation system are studied. As a reference, non-hydrophobised and non-insulated walls are analysed. The paper is organised as follows. Section 2 first describes the field test setup and the applied measurement techniques. Next, in Section 3 a selection of the logged data is presented and analysed. In Section 4, a special focus is put on the impregnation depth in the masonry. Finally, in Section 5 the main conclusions are drawn.

2 Field Test Setup

2.1 Test Walls

To study the impact of hydrophobisation on internally insulated walls, six 1.5-stone thick masonry test walls of approximately 32 cm thick, 0.6 m wide and 2.7 m high were constructed in two south-west oriented wall frames of the VLIET test building of KU Leuven (Figure 1a).

The masonry assemblies were masoned by use of Vandersanden Robusta bricks ($A_{cap} \approx 0.61$ kg/(m^2.s$^{0.5}$)) and lime mortar (ratio: 12.5 kg Saint-Astier NHL3.5, 50 kg River sand 0/2, 10 litres water; $A_{cap} \approx 0.26$ kg/(m^2.s$^{0.5}$) for mould cured mortar). Between the different test walls a barrier was provided, such that the hygrothermal behaviour of the test walls was not affected by the adjacent test walls. The construction of the test walls was finalised by the end of August 2017, after which a drying period took place. On October 23th 2018, three of the six test walls (Figure 1b) were hydrophobised by use of Silres® SMK2100 from Wacker Chemie AG. An impregnation depth of 3 cm in the bricks was pursued, for which per m^2 wall 6.9 litres of a 10 vol% hydrophobic agent solution was applied by spraying. The rain load on the test setup was measured via two wall-mounted WDR gauges (Figure 1b,c), with a collection area of 0.2 m x 0.2 m, as used by Blocken and Carmeliet (2006). To ease a comparison between the wall's hygrothermal performance and the WDR, the WDR load measured by the top WDR gauge is shown together with the results (Figure 4a).

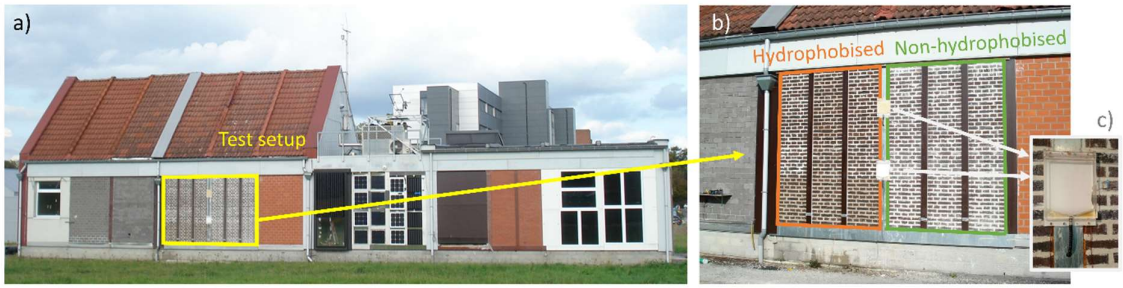

Figure 1. Outside view of the field test setup: (a) south-west oriented side of the VLIET-test building, (b) hydrophobised and non-hydrophobised masonry test walls with (c) wind-driven rain gauges.

On the inside, two test walls were provided with a vapour tight XPS interior insulation system, while two other test walls had a capillary active calcium silicate (CaSi) interior insulation system. Both systems were built up of a 10 cm thick insulation board which was fully adhered to the masonry by use of a glue mortar. As an interior finish, the XPS-system and the CaSi-system were provided with a gypsum board and plaster layer, respectively. The application of the interior insulation systems was performed in the second half of December 2018. The remaining two test walls had no interior insulation system, and thus acted as reference walls. An overview of the six test cases is given in Table 1. In each of the test walls, two wooden beam ends were embedded in the masonry (Figure 2). The upper wooden beam ends were in contact with a mortar layer, whereas for the lower wooden beam ends an air gap was present at all sides except for the bottom of the wooden beam end. At the room side, the end of the wooden beams were covered with bituminous paint, avoiding vapour diffusion via the longitudinal wood direction. To prevent convective moisture transport, as discussed in

(Vereecken and Roels, 2018), the gap between the wooden beam and the insulation system was sprayed up with flexible PUR-foam and the connection with the interior surface was sealed with an airtight tape. After all, also in hygrothermal studies including a wind-driven rain exposure (Kopecký *et al.*, 2019) an airtight sealing of the beam junction has been put forward.

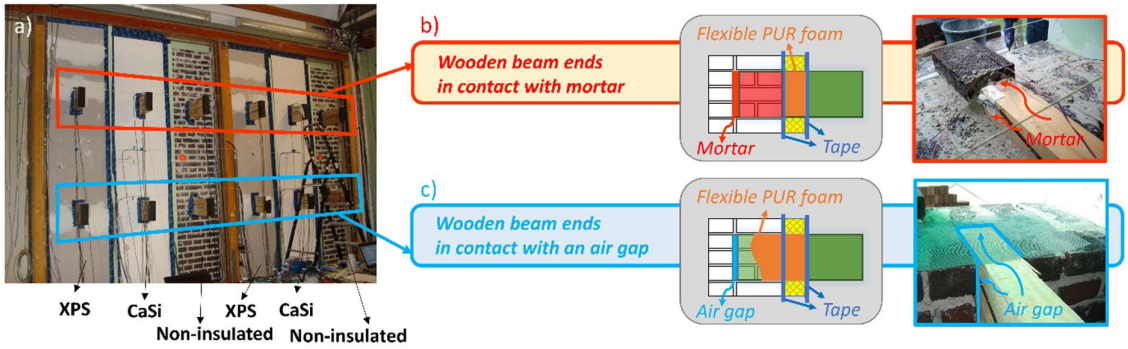

Figure 2. Inside view of the test walls: (a) global overview of the internally insulated and non-insulated test walls with embedded wooden beam ends, (b) wooden beam end in contact with mortar and (c) wooden beam end in contact with an air gap.

Table 1. Overview of the test walls.

Label	Hydrophobisation?	Interior insulation system
NH-XPS	No	XPS
NH-CaSi	No	CaSi
NH-Non	No	Non-insulated
H-XPS	Yes	XPS
H-CaSi	Yes	CaSi
H-Non	Yes	Non-insulated

2.2 Measurement Techniques

The temperature and the relative humidity in the test walls were measured by use of in-house calibrated Thermo Electric Type T (class 1) thermocouples and Honeywell HIH-4021 humidity sensors, with an accuracy of +/- 0.2°C and +/- 2% RH. Furthermore, in-house made moisture pins, measuring the electrical resistance, were used to analyse the moisture conditions at the back of the wooden beam ends, in the mortar in the masonry, in the glue mortar and in the calcium silicate. It is well known that the electrical resistance of a material depends on the material's moisture content, as moisture is a good electrical conductor. The lower the electrical resistance measured in a material, the higher the moisture content of the material. For a more in depth description on the electrical resistance method, the reader is referred to (Otten *et al.*, 2017). At half height of the test walls, additionally a heat flux sensor was glued at the warm side of the masonry. The position of the different sensors is shown in Figure 3. For the moisture pins a preliminary calibration took place, of which an example for the in-situ mortar moisture pins is given in Figure 3c.

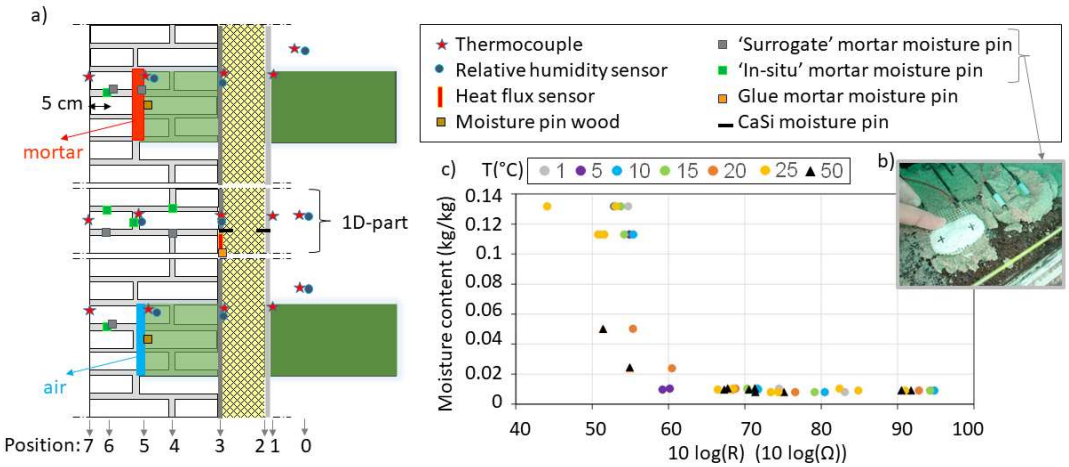

Figure 3. (a) Position of the thermocouples, humidity sensors, moisture pins and heat flow sensor indicated for the wall with CaSi, (b) in-house made surrogate (left) and in-situ (right) mortar moisture pins, (c) preliminary calibration curve for the in-situ mortar moisture pin.

3 Results

Hourly-averaged data are used for the analysis of the hygrothermal performance of the test walls. In what follows, the measurements achieved in the period from June 2018 till the end of October 2019 are shown. Thus, a period in which the walls were all non-hydrophobised and non-insulated is included, showing the similar initial moisture level for the six walls. In the legend of the graphs, from the start however, these walls are indicated by their final state of hydrophobisation and interior insulation system. Focus is put on the moisture conditions in the mortar layer in the 1D-part of the masonry, as measured by the in-situ mortar moisture pins, and on the moisture conditions of the wooden beam ends. To analyse the data measured by the moisture pins, it is important to keep in mind the inverse relation between electrical resistance and moisture content. A lower electrical resistance represents a higher moisture content.

Furthermore, a preliminary calibration of the in-situ mortar moisture pins (Figure 3c) showed an electrical resistance above 60 x 10 log(Ω) to correspond to a similar moisture content. The electrical resistance at which this phenomenon occurs can however slightly vary depending on the material the moisture pins are embedded in (Brischke *et al.*, 2008). Hence, at this point, the moisture pins don't allow an absolute comparison of the measurement data in the lower moisture range (above an electrical resistance in the range of 60 x 10 log(Ω)).

3.1 Moisture Conditions in the 1D-Masonry Part

Figure 4b, c and d show the electrical resistance as measured by the in-situ mortar moisture pins in the middle (1D) part of the test walls. Additionally, the relative humidity at Position 5 is shown (Figure 4e). Both the relative humidity and the electrical resistance show a drying behaviour in the period before the water repellent agent was applied. When applying the hydrophobisation, for the hydrophobised walls an abrupt drop in electrical resistance is shown at Position 6, which is closest to the outer surface. After this, the electrical resistance starts increasing again slowly, which indicates a drying of this outer masonry region. For Position 5,

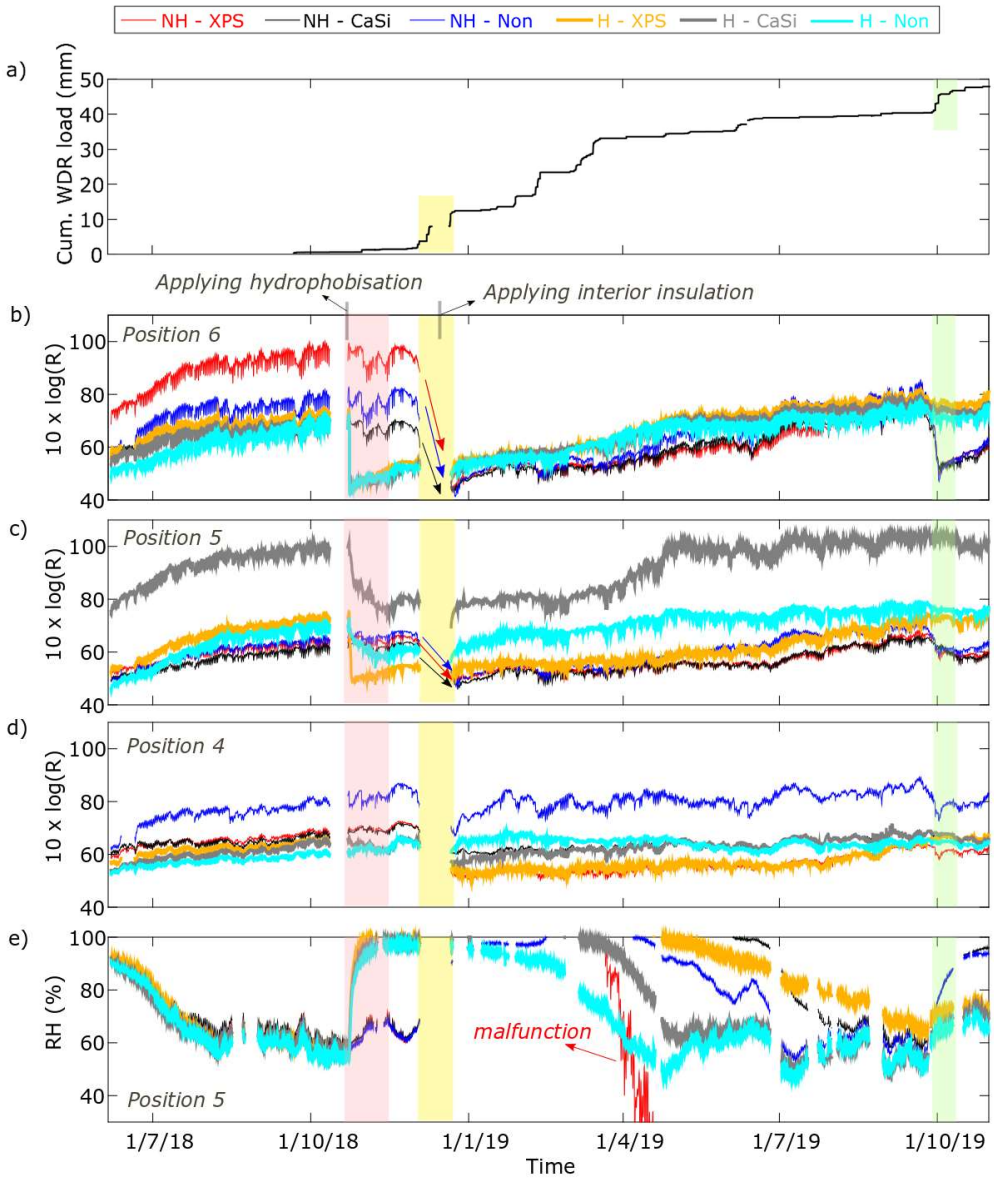

Figure 4. (a) Cumulative wind-driven rain load measured by the top WDR gauge, (b,c,d) electrical resistance measured by the moisture pins in the 1D-part of the walls for (b) Position 6, (c) Position 5 and (d) Position 4, (e) relative humidity measured in the 1D-part at Position 5 (see Figure 3 for an indication of the positions).

a decrease in electrical resistance occurs over a longer time period after the hydrophobisation (pink rectangle), which can be attributed to an inward redistribution of the water used for the water repellent solution. For the hydrophobised wall with a CaSi-interior insulation system, the measurement data seem to be shifted upward compared to the other walls. No explanation is found for this behaviour and a malfunctioning of the moisture pin is assumed; though the decreasing trend is also here visible. For the three hydrophobised walls, the inward redistribution indicated by the moisture pins is confirmed by the relative humidity sensor at

Position 5 (Figure 4e). Deeper in the wall (Position 4), no distinct changes are found during or shortly after the application of the hydrophobisation (Figure 4d).

In December 2018 (yellow rectangle), a reverse behaviour can be observed. In a part of this period the sensors were disconnected to install the interior insulation systems. Though, a comparison of the data before and after this interruption shows, especially for Position 6, a strong decrease in electrical resistance for the three non-hydrophobised walls. This can be attributed to wind-driven rain absorbed by the walls (see Figure 4a). The electrical resistance measured in the hydrophobised walls remains substantially the same. A similar behaviour is found in October 2019. Other WDR loads (*e.g.* in February/March 2019) are less visible, since the moisture level in the wall is already high at that time.

The impact of the interior insulation systems is visible in the relative humidity at Position 5 (Figure 4e). In spring and summer, a decrease in relative humidity is observed, which occurs first for the hydrophobised non-insulated wall, followed by the hydrophobised wall with the CaSi-system and the non-hydrophobised non-insulated wall. Next, the relative humidity in the hydrophobised wall with XPS starts decreasing, but this occurs slower than found for the non-hydrophobised wall with the CaSi-system. The relative humidity sensor in the non-hydrophobised wall with XPS showed some malfunctioning due to the high moisture load.

3.2 Moisture Conditions at the Wooden Beam Ends

Figure 5 shows the relative humidity at Position 5 on the wooden beam ends. For the beam ends in contact with mortar (Figure 5a) the relative humidity at the beginning of June 2018 is found to be above 90%. The test walls are at that moment still non-hydrophobised and non-insulated, and hence show a relative humidity that is in close agreement for the different walls. During the next half year, a drying out takes place until a quasi-equilibrium is found close above 60% RH. For the lower beam ends provided with an air gap between beam and masonry (Figure 5b), the relative humidity level is found to be between 40 and 65% during this entire period.

For the period after January 2019, for both the upper and lower wooden beam end an increase

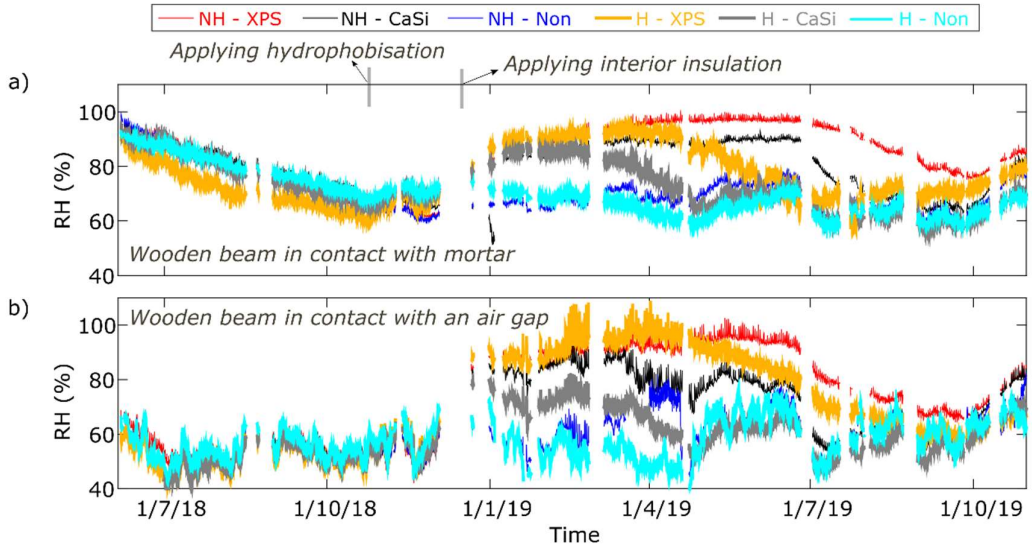

Figure 5. Relative humidity at Position 5 (see Figure 3) at (a) the upper and (b) the lower wooden beam end.

in relative humidity is measured for the walls with interior insulation. This can be partially explained by the lower wall temperature. Apart from this, also a higher moisture content in the wall as indicated by the moisture sensors (Figure 4d) can contribute to this, especially for the upper wooden beam which is in contact with mortar. During spring and summer, the relative humidity starts decreasing again. Also here, the slowest decrease is found for the non-hydrophobised wall with XPS and the fastest for the hydrophobised system with CaSi. The relative humidity level for the non-insulated walls remains rather stable over the entire period.

4 Analysis of the Impregnation Depth

In Section 3, the hydophobisation process was shown to induce a large increase in moisture content in the mortar at 5 cm from the outer surface of the masonry (Position 6). In order to achieve a view on the extent to which also the hydrophobic agent was transported in the wall, the impregnation depth was further analysed via an additional laboratory test setup. Thereto, a small test wall masoned with the same type of bricks and mortar as applied in the VLIET test setup and hydrophobised in a similar way (Figure 6a) was built. This wall was cut in half (Figure 6b) and tilt such that the center plane became a horizontal plane on which the penetration depth of the hydrophic agent could be analysed via the droplet method. Water droplets were dropped on the surface by use of a pipette and the contact angle of the droplet was analysed. For the bricks, three zones were detected (Figure 6c). In the zone closest to the outer (hydrophobised) surface a fully hydrophobised effect was observed. Droplets with a contact angle larger than 90° were clearly noticed (Figure 6e). The impregnation depth in the bricks seemed to be larger than the pursued 3 cm, which might be due to the dynamic way of spraying the hydrophobisation. This zone passed into a second zone where the droplets collapsed and were next absorbed slowly by the brick layer (Figure 6d). Deeper in the wall the bricks seemed not impregnated. After this droplet measurement, a small brick-mortar sample (Figure 6f) was sawn out of the middle surface of the smaller test wall. The non-hydrophobised surface was brought in contact with a water level, while the moisture content in the test sample was analysed by the X-ray projection technique (Roels and Carmeliet, 2006). At the end of this experiment, the moisture front had reached the boundary of the first impregnation zone (figure 6g). In the mortar layer, the impregnation depth was found to be much smaller (1 to 2 cm). Hence, the increase in moisture content observed in Section 3 is expected to be attributed to liquid transport only. The active ingredient is not transported with it to the position of the moisture pins in the mortar.

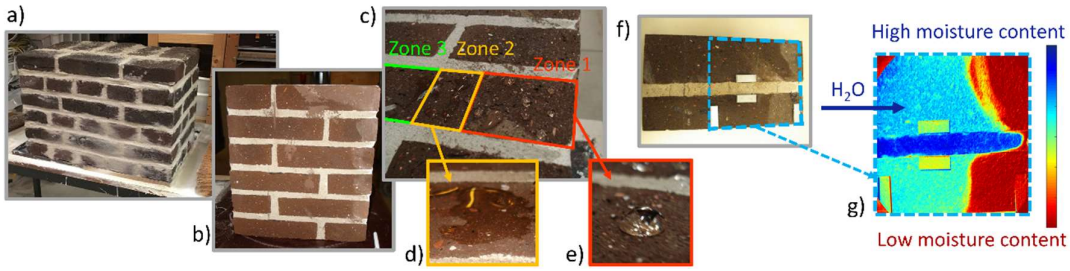

Figure 6. Study on the impregnation depth for a small semi-duplicate test wall: (a) the test wall, (b) test wall vertically cut in half, (c,d,e) droplets and collapsed droplets indicating different hydrophobised zones, (f) test sample sawn out the test wall for the X-ray test with metal dummy's as position references, (g) moisture content measured by the X-ray projection method after bringing the non-hydrophobised surface in contact with water.

5 Discussion and Conclusions

Preliminary results of a field study on the impact of interior insulation and hydrophobisation on the hygrothermal performance of massive masonry walls with embedded wooden beam ends has been presented. In-house made moisture pins yielded valuable information on the moisture transfer in the masonry during and after spraying the water repellent agent. After all, installing RH sensors in the wet mortar entails a risk on malfunction of the sensors and is not obvious in the high moisture range. A further calibration of the moisture pins is however required to make a conversion to the moisture content and a further analysis of the measurements possible.

In the current study, an increased moisture level was induced during the hydrophobisation process. A drying period was needed to again reduce the moisture level near the outer surface.

When disregarding the period shortly after applying the water repellent agent, hydrophobisation showed a positive impact on the wall's hygric performance. Deeper in the wall, near the wooden beams ends, the highest relative humidity was observed for the non-hydrophobised wall with a vapour tight interior insulation system. The non-insulated test walls showed the lowest relative humidity, regardless of the presence of a hydrophobisation. Further research will include an analysis over a longer time period, to exclude the initial influence of the application of the water repellent agent, and this for the total set of sensors and moisture pins embedded in the test walls.

Acknowledgements

The results within this paper have been partially obtained within the EU Horizon 2020 RiBuild project (Project ID 637268). Evy Vereecken is a postdoctoral fellow of the Research Foundation (FWO) - Flanders, Belgium (FWO project 12J5219N). These financial supports are gratefully acknowledged. The authors are very grateful to Wim Bertels, Patricia Elsen, Bernd Salaets and Jimmy Van Criekingen for their dedicated contributions in realising these measurements in practice.

ORCID

Evy Vereecken: https://orcid.org/0000-0003-2700-7969
Hans Janssen: https://orcid.org/0000-0002-8315-3955
Staf Roels: http://orcid.org/0000-0002-1156-8553

References

Blocken, B. and Carmeliet, J. (2006). On the accuracy of wind-driven rain measurements on buildings. *Building and Environment, 41(12)*, 1798-1810. doi: 10.1016/j.buildenv.2005.07.022

Otten, K., Brischke, C. and Meyer, C. (2017). Material moisture content of wood and cement mortars – electrical resistance-based measurements in the high ohmic range. *Construction and Building Materials, 153*, 640-646. doi: 10.1016/j.conbuildmat.2017.07.090

Kopecký, P., Staněk, K., Bureš. M., Richter, J., Ryparová, P. and Tywoniak, J. (2019). Experimental investigations of wooden beam ends in masonry with interior insulation: Measured data in real-scale experimental walls exposed to semi-continental climatic conditions. *Journal of Building Physics, 43(3)*, 147-170. doi: 10.1177/1744259119867461

Roels, S. and Carmeliet, J. (2006). Analysis of moisture flow in porous materials using microfocus X-ray radiography. *International Journal of Heath and Mass Transfer, 49*, 4762-4772. doi: 10.1016/j.ijheatmasstransfer.2006.06.035

Vereecken, E., Van Gelder, L., Janssen, H. and Roels, S. (2015). Interior insulation for wall retrofitting – A probabilistic analysis of energy savings and hygrothermal risks. *Energy and Buildings, 89,* 231-244. doi: 10.1016/j.enbuild.2014.12.031

Vereecken, E. and Roels, S. (2018). Wooden beam ends in combination with interior insulation: An experimental study on the impact of convective moisture transport. *Building and Environment*, *148*, 524-534. doi: 10.1016/j.buildenv.2018.10.060